One-Step Synthesis of Core(Cr)/Shell(γ-Fe_2O_3) Nanoparticles

Jriuan Lai,[†,▽,○] Kurikka V. P. M. Shafi,[†,▽,#] Abraham Ulman,*[,†,▽,×] Katja Loos,[‡,▽] Ronit Popovitz-Biro,[§] Yongjae Lee,[∥] Thomas Vogt,[∥] and Claude Estournès[⊥,◇]

Othmer Department of Chemical and Biological Sciences and Engineering, Polytechnic University, 6 Metrotech Center Brooklyn, New York 11201, Polymer Chemistry and Materials Science Center, Department of Mathematics and Natural Sciences, University of Groningen, Nijenborgh 4, 9747AG Groningen, The Netherlands, Department of Materials and Interfaces, The Weizmann Institute of Science, Rehovot, Israel, Physics Department, Brookhaven National Laboratory, P.O. Box 5000, Upton, New York 11973, Institut de Physique et Chimie des Matériaux de Strasbourg, UMR 7504, 23 rue du Loess−BP 43−67034 Strasbourg, France, and The NSF Garcia MRSEC for Polymers at Engineered Interfaces

E-mail: aulman@duke.poly.edu

Interest in nanoparticles is stimulated from their technological importance, as they exhibit unique electrical, optical, and magnetic properties, which differ from their respective bulk.[1−5] Magnetic nanoparticles with the size of 2−10 nm are particularly important because they are potentially useful in terabit magnetic storage, as carriers for biochemical complexes, as MRI contrast enhancing agents, etc.[6] Core/shell nanoparticles, produced by various methods, can be applied for sensing, for high-density information storage, etc.[7c,8] Here we present the one-step synthesis of core/shell magnetic nanoparticles and their characterization.

The nanoparticles were prepared by adding 0.21 mL of $Fe(CO)_5$ and 39.98 mg pf of $Cr(CO)_6$ to 100 mL of degassed mesitylene (preheated to 70 °C). The molar ratio surfactant:carbonyls:solvent was 1:100:40000, and 9:1 for $Fe(CO)_5$:$Cr(CO)_6$. After stirring for 5 min, 226 mg of the polymer surfactant, Pluronic F127, was added. The temperature was then raised to reflux (∼165 °C) for 24 h under reducing environment (5% H_2; 95% Ar). After cooling to room temperature, the resulting precipitate was collected by centrifugation, washed with toluene, and dried under vacuum.

The TEM image (Figure 1) shows the particles have spherical shape. The insert histogram shows particles size distribution of 13 ± 4 nm. The narrow size distribution is in good agreement with the magnetic measurements (Supporting Information). A small group of particles with the diameter 4−6 nm might be the result of decomposition at lower temperature.[9] An interesting feature in the image (see arrows) is a small dot inside of each particle core/shell structure. This suggests that the particles are not homogeneous and the material of the core differs from that of the shell.

The synchrotron powder XRD pattern (Supporting Information) of nanoparticles was fitted to more than one index, which supports finding heterogeneous particles from the TEM image. Apparently, the majority of the sample matches the γ-Fe_2O_3 crystal structure. However, since both Fe and Cr have the same crystal structure with different lattice constants, it is hard to determine what is the metal pattern at this point.

† Polytechnic University.
‡ University of Groningen.
§ The Weizmann Institute of Science.
∥ Brookhaven National Laboratory.
⊥ Institut de Physique et Chimie des Matériaux.
▽ The NSF Garcia MRSEC for Polymers at Engineered Interfaces.
○ Current address: Department of Bioengineering, University of Washington, Seattle, WA 98195.
Current address: Infineon Technologies NA, 2070 Route 52, Zip 130, Hopewell Junction, NY 12533.
× Current address: Department of Chemistry, Bar-Ilan University, Ramat-Gan 52900, Israel.
◇ Current address: CIRIMAT UMR 5085, 118 route de Narbonne, 31062 Toulouse Cedex 04, France.

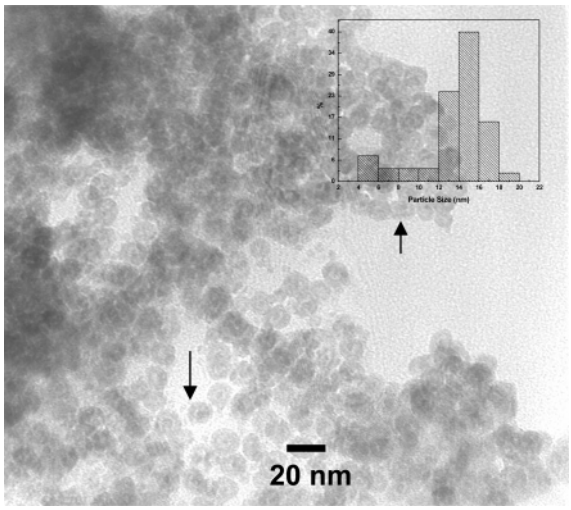

Figure 1. TEM image of the core/shell nanoparticles. (Inset) Histogram prepared by measuring ca. 200 nanoparticles.

The Mössbauer spectra (Supporting Information) are in good agreement with the results from SQUID (Supporting Information). They are characterized by a doublet at room temperature and by a sextet at 4.2 K. The change is due to the fact that the magnetic moment in the particles is random at room temperature, and they therefore behave like paramagnetic while there is an internal field at the blocked state at low temperatures, which generates a Zeeman splitting of the levels. At 295 K one observes two components: Fe^{3+} (96.57%) exhibiting superparamagnetic behavior and a small impurity of Fe^{2+} (3.43%). At 77 K we also observe Fe^{3+} and Fe^{2+}, but in lower amounts. Since almost all of the Fe atoms are trivalent, the crystal structure can be confirmed as γ-Fe_2O_3. Notice that no Fe^0 could be detected, which indicates that the metal component from the XRD pattern is Cr. To ascertain the exact structure of the core/shell nanoparticles, we have carried out HR-TEM, EELS, and iron mapping.

Nanoparticles of approximately 12 nm in diameter were imaged by the HR-TEM, showing a high contrast core of about 4.5 nm in diameter (Figure 2a). The electron energy loss spectrum (EELS) (Figure 2d) clearly shows three edges: the O K, Cr L2, and Fe L2. Quantification of the EELS, from such particles, revealed an Fe: Cr ratio of about 9:1, which is in good agreement with the stoichiometry of the reaction. However, there is more than one source of oxygen, polymer, and oxide layers, so that the amount of oxygen varied at different spots of the sample. This result suggests that the sample is not homogeneous which is in good

10.1021/ja0443225

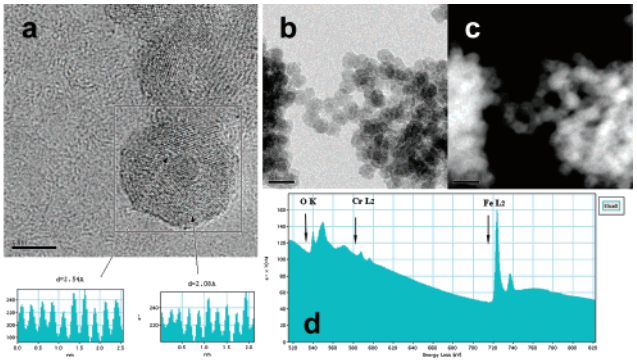

Figure 2. (a) HR-TEM image of a core/shell nanoparticle with intensity profile of the lattice fringes, (b) zero loss image, (c) iron mapping, (d) EELS of the core/shell nanoparticles.

agreement with the TEM and XRD results. The EELS analysis of a single core/shell particle was performed in nanoprobe mode. One measurement on the entire particle resulted in an O:Cr:Fe ratio of 10:1.1:9.3, while a second measurement performed with the electron probe on the shell resulted in an O:Cr:Fe ratio of 10:0.3:6.3. This suggests that the shell in this particle is Fe_2O_3, which is in good agreement with the XRD pattern and Mössbauer spectra, so that the core should be Cr.

Lattice fringe could be observed both in the core and in the shell of the particles. The shell seems to consist of randomly oriented crystalline grains. Fast Fourier transform performed on such images gave several characteristic spots corresponding approximately to the *d* spacing: 2.97, 2.56, 2.10, and 1.67 Å. However, not all four spots appear in every particle analyzed. For example, in Figure 2a, the *d* spacings measured in the two designated areas are 2.54 and 2.08 Å that can be assigned to Fe_3O_4 or $FeCr_2O_4$. Mössbauer spectra (Supporting Information) also suggest the existence of Fe_3O_4. The possibility of $FeCr_2O_4$ is excluded since these lattice fringes were observed in the shell where Cr does not reside.

Energy-filtered imaging was performed by using a 40 eV energy window (708−748 eV) around the iron edge, to form an iron map. The regions containing Fe are bright, while other regions are dark in such an image. Thus, in the Fe mapping performed on the core/shell nanoparticles, shown in Figure 2, b and c, the donut-shaped bright structures indicate that the Fe constitutes the shell, which supports the finding from EELS analysis, while the dark region (particle core) in the core is probably the Cr.

On the basis of the result of EELS, Mössbauer spectra, and HR-TEM, the materials balance calculation (Supporting Information) was performed to estimate the density of particle core. The result shows there is no oxide in the particles core. Since Mössbauer spectra show no trace amount of Fe^0, we can conclude the particle core is Cr.

The decomposition temperature of $Fe(CO)_5$ (∼60 °C)[10a] is much lower than that of $Cr(CO)_6$ (∼130 °C);[10b] thus, the decomposition reaction rate of $Fe(CO)_5$ should be faster than that of $Cr(CO)_6$ at ∼165 °C. Therefore, Fe should be formed before Cr, and the resulting particles should be Fe core and Cr shell. However, on the basis of the above results, they are confirmed to be Cr core and γ-Fe_2O_3 shell. To fully understand this result, the reaction mechanism (Supporting Information) is crucial. These nanoparticles were prepared in a one-step reaction from the carbonyl precursors. Due to the much lower decomposition temperature, $Fe(CO)_5$ was decomposed faster than $Cr(CO)_6$ and forms a small amount of Fe clusters, which were then used as the catalysts[11] to accelerate the decomposition of $Cr(CO)_6$. Combine this with the consideration that the amount of $Cr(CO)_6$ is only 10%, and thus, the formation of a Cr core presumably results from accelerated decomposition of $Cr(CO)_6$, catalyzed by the Fe clusters. The Cr core is then used as the nucleation seed to form an Fe shell layer. Since particles of this size cannot stay stable as metal, the Fe shell oxidized to γ-Fe_2O_3, which protects the core from oxidation; in addition Cr has strong oxidation resistance. Therefore, the particle core stayed as Cr.

In conclusion, by mixing $Fe(CO)_5$ and $Cr(CO)_6$ in the 9:1 ratio, we have successfully synthesized core/shell nanoparticles 13.5 nm in diameter, with uniform spherical shape and narrow distribution. The core/shell structure is formed by Fe^0 clusters catalyzing the decomposition of $Cr(CO)_6$. TEM image reveals the heterogeneous nature (core/shell structure), which is in good agreement with the synchrotron powder XRD pattern. The pattern shows more than one crystal structure in the materials. One was identified as γ-Fe_2O_3 and the other as a metal crystal structure. Mössbauer spectra, which support the superparamagnetic behavior determined by H−M measurement, do not show any traceable amount of Fe^0. This suggests that the metal component might be Cr. EELS analysis and iron mapping suggest controlled stoichiometry and confirm a core made of Cr and a shell made of γ-Fe_2O_3.

Acknowledgment. This work was funded by the NSF through the MRSEC for Polymers at Engineered Interfaces. Research carried out in part at beamline X7A the NSLS at BNL is supported by the U.S. DOE (DE-AC02-98CH10886). K.L. thanks the AvH foundation for financial support. J.L. thanks the financial support from Robert Tsao Endowment Fellowship.

Note Added after ASAP Publication: In the version published on the Internet April 5, 2005, the current address for one of the authors was incorrect. In the final version, published April 6, 2005, and in the print version this is correct.

Supporting Information Available: Details of characterization techniques, magnetic measurements, and materials balance calculation. This material is available free of charge via the Internet at http://pubs.acs.org.

References

(1) Bradley, J. S.; Hill, E.; Leonowicz, M. E.; Witzke, H. *J. Mol. Catal.* **1987**, *41*, 59−74.
(2) Murray, C. B.; Kagan, C. R.; Bawendi, M. G. *Science* **1995**, *270*, 1335−1338.
(3) Alivisatos, A. P. *Science* **1996**, *271*, 933−937.
(4) LizMarzan, L. M.; Giersig, M.; Mulvaney, P. *Chem. Commun.* **1996**, 731−732.
(5) Caruso, F. *Adv. Mater.* **2001**, *13*, 11−13.
(6) Sun, S. H.; Murray, C. B.; Weller, D.; Folks, L.; Moser, A. *Science* **2000**, *287*, 1989−1992.
(7) (a) Park, J. I.; Kim, M. G.; Jun, Y. W.; Lee, J. S.; Lee, W. R.; Cheon, J. *J. Am. Chem. Soc.* **2004**, *126*, 9072−9078. (b) Pastoriza-Santos, I.; Koktysh, D. S.; Mamedov, A. A.; Giersig, M.; Kotov, N. A.; Liz-Marzan, L. M. *Langmuir* **2000**, *16*, 2731−2735. (c) Ravel, B.; Carpenter, E. E.; Harris, V. G. *J. Appl. Phys.* **2002**, *91*, 8195−8197. (d) Kickelbick, G.; Holzinger, D.; Brick, C.; Trimmel, G.; Moons, E. *Chem. Mater.* **2002**, *14*, 4382−4389. (e) Kuhn, L. T.; Bojesen, A.; Timmermann, L.; Nielsen, M. M.; Morup, S. *J. Phys.: Condens. Matter* **2002**, *14*, 13551−13567. (f) Zeng, H.; Li, J.; Wang, Z. L.; Liu, J. P.; Sun, S. H. *Nano Lett.* **2004**, *4*, 187−190. (g) Teng, X. W.; Black, D.; Watkins, N. J.; Gao, Y. L.; Yang, H. *Nano Lett.* **2003**, *3*, 261−264.
(8) Nayral, C.; Viala, E.; Fau, P.; Senocq, F.; Jumas, J. C.; Maisonnat, A.; Chaudret, B. *Chem.—Eur. J.* **2000**, *6*, 4082−4090. (b) Zhou, W. L.; Carpenter, E. E.; Lin, J.; Kumbhar, A.; Sims, J.; O'Connor, C. J. *Eur. Phys. J. D* **2001**, *16*, 289−292. (c) Yu, M. H.; Devi, P. S.; Lewis, L. H.; Oouma, P.; Parise, J. B.; Gambino, R. J. *Mater. Sci. Eng., B* **2003**, *103*, 262−270.
(9) Hyeon, T. *Chem. Commun.* **2003**, 927−934.
(10) (a) Friedrich, G.; Ebenhöch, F. L.; Kühborth, B. *Ullmann's Encyclopedia of Industrial Chemistry*, 7th ed.; Wiley VCH: New York, 2004. (b) *CRC Handbook of Chemistry and Physics*, 85th ed.; CRC Press: Cleveland, 2004.
(11) (a) Takeuchi, K. J.; Marschilok, A. C.; Bessel, C. A.; Dollahon, N. R. *J. Catal.* **2002**, *208*, 150−157. (b) Mahajan, D.; Gutlich, P.; Stumm, U. *Catal. Commun.* **2003**, *4*, 101−107. (c) Choi, H. C.; Kundaria, S.; Wang, D. W.; Javey, A.; Wang, Q.; Rolandi, M.; Dai, H. J. *Nano Lett.* **2003**, *3*, 157−161.

JA0443225

1 Characterization Techniques

1.1 Synchrotron Powder X-ray Diffraction

Experiments were performed at the beamline X7A of the National Synchrotron Light Source (NSLS) at Brookhaven National Laboratory with a linear position-sensitive detector gating electronically on the Kr-escape peak. Monochromatic x-rays were obtained using a water-cooled Ge111 channel cut monochromator. The instrumental resolution in this setup, $\Delta d/d$, is ~ 10^{-3}. The sample was contained in an unsealed 0.3 mm capillary, which was rotated at a frequency of roughly 1 Hz to reduce preferred sample orientation effects.

1.2 Transmission Electron Microscopy (TEM)

Nanocrystal size and morphology were investigated using a Phillips CM-12 Transmission Electron Microscope (100 KeV). Nanocrystals suspended in toluene, were deposited onto a carbon stabilized Formvar-coated copper grid (400 mesh) and allowed to dry.

1.2.1 Magnetic measurements

Magnetic data of the solid samples were collected with a Quantum Design SQUID MPMS-XL (AC and DC modes and maximum static field of ± 5 T) both in liquid helium and room temperatures. The temperature dependence of the magnetization was measured in the range 5 - 400K in an applied field of 20 Oe, after cooling in zero magnetic field (ZFC) or by cooling in a field of 20 Oe (FC).

1.3 Mössbauer Spectroscopy

Mössbauer measurements were performed using a constant acceleration HALDER-type spectrometer with a room-temperature ^{57}Co source (Rh matrix) in transmission geometry. The polycrystalline absorbers containing about 10 mg cm^{-2} of iron were used to avoid the experimental widening of the peaks. The spectra at 4.2 and 293 K were recorded using a variable-temperature cryostat. The velocity of the ^{57}Co source was calibrated using pure iron metal as the standard material. The refinement of the Mössbauer spectra showed an important and abnormal widening of the peaks, so that the spectra were fitted assuming a distribution either of quadrupolar splittings or of hyperfine fields.

1.4 HR-TEM and EELS Experimental

Specimens were prepared by touching the dry powder with C/Collodion coated Cu grids. High-resolution transmission electron microscopy measurements were performed on a FEI Tecnai F-30 UT operating at 300kV and equipped with a field emission gun. Energy filtered imaging and electron energy loss spectroscopy (EELS) were performed using Gatan Image Filter (GIF).

2 Magnetic Measurement Results

The magnetic properties of the core/shell nanoparticles were studied by using SQUID at field range of ± 5 T (H-M) and the temperature range from 2 to 300 K (T-M). H-M measurements from SQUID were used to observe the induced magnetization from the materials in the applied field. Figure 1 illustrates the H-M data. The measurements

show no coercivity at room temperature. A hysteresis appears with 1500 Oe, as the coercivity at 5 K. This is the typical H-M behavior for superparamagnetic materials. The magnetization at 5 T is ~ 23 emu/g for measurements at 295 K and 32 emu/g for measurement at 5 K, after the polymer content (60% weight loss by TGA) has been

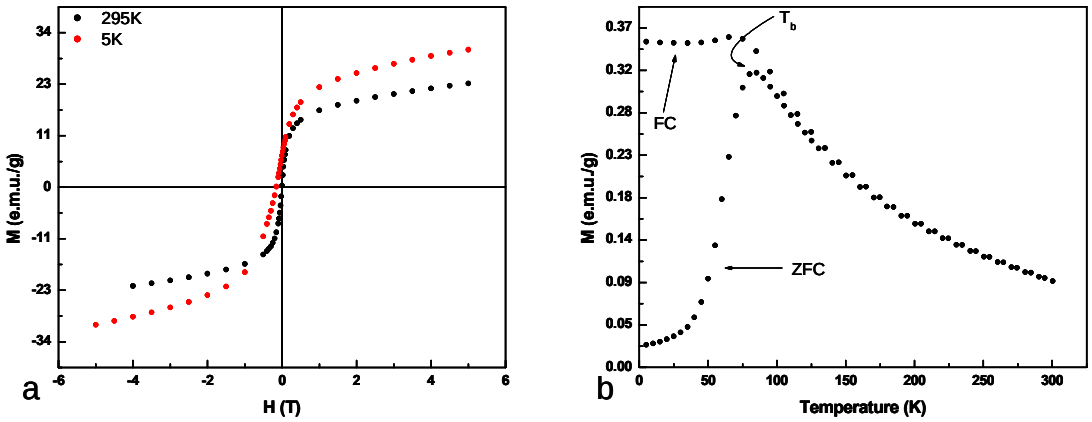

Figure 1. (a) H-M measurements; (b) T-M measurements.

subtracted.

The saturation moment is 76 emu/g for γ-Fe_2O_3 and 210 emu/g for Fe, and Cr is paramagnetic material. The particles size is a possible explanation why the magnetic moment of the sample particles is significantly lower than the literature values. When particles are small, their magnetic order is easier to be randomized, so it is hard to reach the saturation moment. Since the magnetic moment of Fe is much higher than that of γ-Fe_2O_3, this should enhance the overall magnetic moment. However, this is not observed here. This is another evidence suggesting that the metal component in the particle should be Cr and not Fe. From the T-M measurements (Figure 1), the maximum of the ZFC curve shows that T_b is 85 K. The fact that the ZFC and the FC curve overlap above T_b is an indication of a narrow particle size distribution. Overall, the materials behave as typical superparamagnetic materials.

3 Synchrotron Powder X-Ray Diffraction

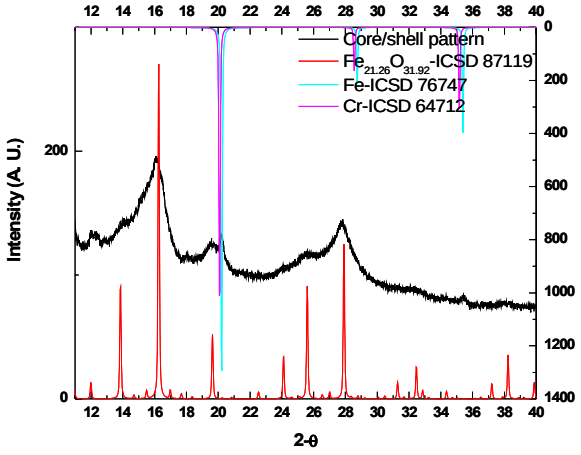

Figure 2. Synchrotron powder XRD pattern of the sample.

4 Mössbauer Spectroscopy Results

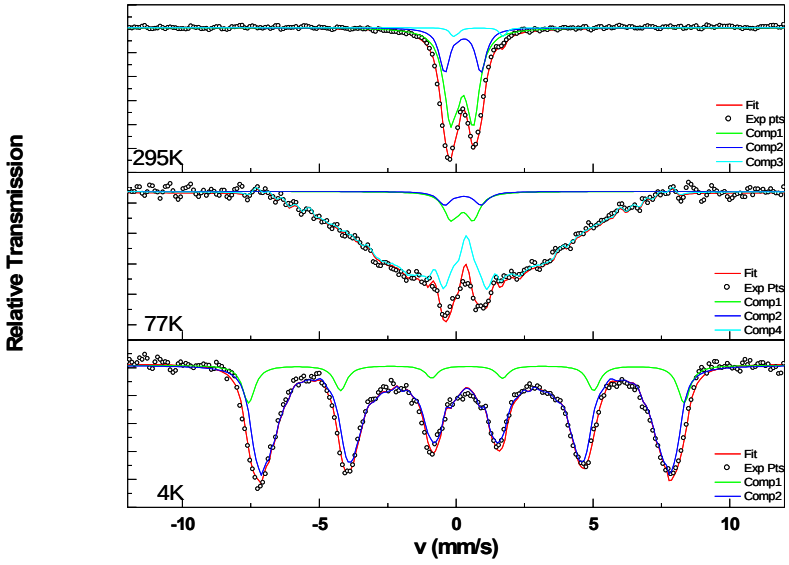

Figure 3. Mössbauer spectrum.

5 Materials Balance Calculation

The molecular weight, *M.W.*, of Cr and Fe are

$M.W._{Cr} = 52.0$ and $M.W._{Fe} = 55.8$.

The density, ρ, of Fe_2O_3, Fe_3O_4 and Cr are

$\rho_{Fe_2O_3} = 5.24\,{}^{g}\!/_{cm^3}$, $\rho_{Fe_3O_4} = 5.10\,{}^{g}\!/_{cm^3}$, and $\rho_{Cr} = 7.19\,{}^{g}\!/_{cm^3}$.

The radius, *r*, of particle, core, and shell are

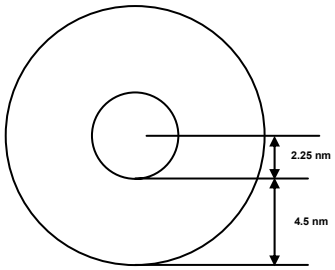

$r_{particle} = 6.75nm$, $r_{core} = 2.25nm$, and $r_{shell} = 4.5nm$.

The volume, *V*, of particle, core and shell are

$V_{partricle} = \frac{4}{3}\pi r_{particle}^3 \approx 1288nm^3$, $V_{core} = \frac{4}{3}\pi r_{core}^3 \approx 47nm^3$, and

$V_{shell} = V_{particle} - V_{core} = 1241nm^3$.

The results of Mössbauer spectra are

Fe^{3+} = 96.57% and Fe^{2+} = 3.43%.

EELS

Element Region	Cr	Fe
Particle	1.1	9.3
Shell	0.3	6.3

This is atomic ratio and needs to be converted to weight basis, so the result is as follows

Region \ Element	Cr	Fe
Particle	57.2	518.94
Shell	15.6	351.54

Assumption: Cr only exists as metal form.

Based on Mössbauer spectra, there is small amount of Fe^{2+}, which is the result of Fe_3O_4. From this we can calculate the portion of Fe_3O_4 and Fe_2O_3. In the from of Fe_3O_4, Fe^{2+}:Fe^{3+} = 1:2. It takes two Fe^{3+} to have Fe_2O_3. Therefore, the ratio Fe_3O_4:Fe_2O_3 is $3.43 : {}^{96.57-2\times3.43}\!/_{2}$. The density of the particle, $\rho_{particle}$, is

$$\rho_{particle} = \frac{57.2}{57.2+518.94}\rho_{Cr} + \frac{518.94}{57.2+518.94}\frac{3.43}{3.43+{}^{96.57-2\times3.43}\!/_{2}}\rho_{Fe_3O_4} + \frac{518.94}{57.2+518.94}\frac{{}^{96.57-2\times3.43}\!/_{2}}{3.43+{}^{96.57-2\times3.43}\!/_{2}}\rho_{Fe_2O_3} = 5.42\,{}^{g}\!/_{cm^3},$$

so the weight of the particle, $W_{particle}$, is

$$W_{particle} = \rho_{particle} \times V_{particle} = 6987\times10^{-28}\,g.$$

The density of shell, ρ_{shell}, is

$$\rho_{shell} = \frac{15.6}{15.6+351.54}\rho_{Cr} + \frac{351.54}{15.6+351.54}\frac{3.43}{3.43+{}^{96.57-2\times3.43}\!/_{2}}\rho_{Fe_3O_4} + \frac{351.54}{15.6+351.54}\frac{{}^{96.57-2\times3.43}\!/_{2}}{3.43+{}^{96.57-2\times3.43}\!/_{2}}\rho_{Fe_2O_3} = 5.31\,{}^{g}\!/_{cm^3},$$

so the weight of the shell, W_{shell}, is

$$W_{shell} = \rho_{shell} \times V_{shell} = 6594\times10^{-28}\,g.$$

From the above result we can calculate the weight of core, W_{core}, and its density, ρ_{core}.

$$W_{core} = W_{particle} - W_{shell} = 393\times10^{-28}\,g,$$

so $\rho_{core} = \dfrac{W_{core}}{V_{core}} = 8.36\,{}^{g}\!/_{cm^3} > \rho_{Cr}$.

6 Reaction mechanism of core(Cr)/shell(γ-Fe_2O_3) nanoparticles.

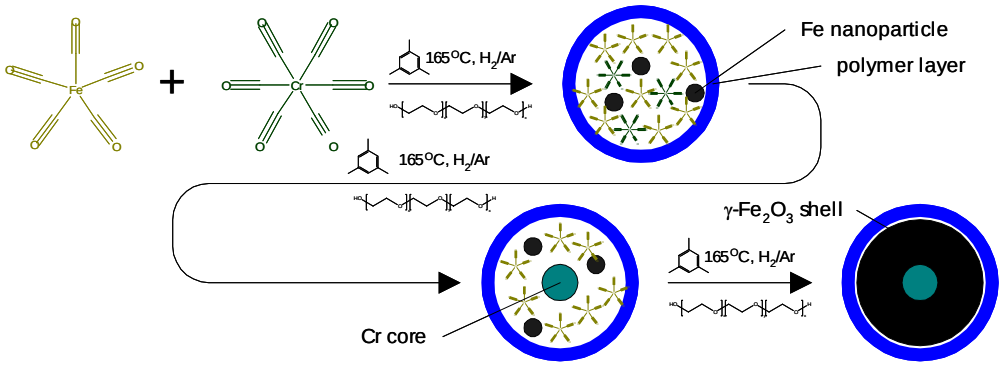

Figure 4. Synchrotron powder XRD pattern of the sample.